A New Discretization Scheme for the Semiconductor Current Continuity Equations

JOSEF F. BÜRGLER, RANDOLPH E. BANK, WOLFGANG FICHTNER, SENIOR MEMBER, IEEE, AND R. KENT SMITH

Abstract—**We describe a new, hybrid finite element method to discretize the continuity equation in semiconductor device simulation. Within each element of a finite element discretization, the current is uniquely determined by nodal values of the density and the potential. We use the integrability condition for a system of partial differential equations to obtain the equations that determine the current within the element. We then satisfy the continuity in the current flow across interelement boundaries in a weak sense. We have found that the method works in any dimension and for (d-dimensional) simplexes as well as for quadrilaterals, bricks, prisms and so on, although we have no proof that it might not break down in particular cases.**

I. Introduction

SINCE the pioneering work by Gummel in 1964 [1], numerical device simulation has experienced an increasingly important role in semiconductor device engineering and technology development. Today, the numerical solution of the semiconductor equations has become a standard technique in device characterization and optimization.

While the numerical solution of the nonlinear partial differential equations has become possible by well-known numerical methods [2], [3], a major problem area has developed in issues concerning the spatial discretization. The increasingly complex two-dimensional structures simulated such as in latch-up investigations [4] render it more and more impossible to rely on optimal (i.e., acute) triangulations. In three dimensions, the situation is even more complex. While several codes based on tensor-product finite-difference codes have found successful applications, they are restricted to rather simple structures such as simple MOSFET's and bipolar devices. An extension of these *brute-force* concepts seems rather unlikely due to the limitations in the number of possible grid points available on todays computing machines.

Until now, the use of irregular grids for complex and "arbitrary" two- or three-dimensional device structures has been severely restricted by strong conditions on the possible angles in the triangulations used [5]. Those conditions arose mainly from the use of a class of discretization methods for the continuity equations. While these so-called *Scharfetter–Gummel* schemes [6] have enjoyed widespread use in most successful semiconductor device codes [7], [8], [3], their applicability is restricted to acute triangulations.

In this paper, we present a new method for the discretization of the semiconductor continuity equations. This discretization can be viewed as a hybrid finite element method, based on physical vector relations of the conduction current. Section III summarizes the device equations used in our work.

In Section IV, we give a short discussion of the original concepts of Scharfetter and Gummel and their extension to more than one dimension in the box method. Furthermore, we identify the known shortcomings of this method as manifested in the obtuse angle problem. The material in Section V brings a derivation of the new method by defining the current in an element. This derivation is based on clear physical assumptions. The section also includes the weak formulation of the continuity equation using the new current expression, and Section VI extends the concepts to allow the inclusion of magnetic field effects.

Section VII illustrates the power of the method with two representative examples, and Section VIII presents our conclusions. In the Appendix, we give more detailed analyses of several important aspects such as the limiting cases of pure diffusion and drift, the relationship with the original Scharfetter–Gummel method, and last but not least, we identify two problem areas related to angle conditions and numerical accuracy.

II. The Semiconductor Equations

In this section we summarize the semiconductor equations as used in this paper. Assuming the validity of the Einstein Relation, the normalized equations can be written as a coupled system of partial differential equations

$$-\Delta u + e^{u-v} - e^{w-u} - N = 0 \tag{1}$$

$$\frac{\partial n}{\partial t} - \nabla \cdot j_n + R = 0 \tag{2}$$

$$\frac{\partial p}{\partial t} + \nabla \cdot j_p + R = 0 \tag{3}$$

Manuscript received July 21, 1988; revised September 29, 1988. The review of this paper was arranged by Guest Editor M. Pinto.

J. Bürgler and W. Fichtner are with the Institut für Integrierte Systeme, Swiss Federal Institute of Technology, CH-8092 Zurich, Switzerland.

R. E. Bank is with the Department of Mathematics, University of California, La Jolla, CA 92093.

R. Kent Smith is with AT&T Bell Laboratories, Murray Hill, NJ 07974.

IEEE Log Number 8826351.

where u, v, and w are the electrostatic potential and the quasi-Fermi potentials for electrons and holes respectively, N is the normalized doping concentration and R the normalized recombination/generation rates. The densities n and p for electrons and holes are related to the electric potential u and the quasi-Fermi potentials v and w in the following way:

$$n = e^{u-v} \tag{4}$$

$$p = e^{w-u}. \tag{5}$$

In (2) and (3), j_n and j_p are the electron and hole currents, respectively. They are given by

$$\begin{aligned} j_n &= -\mu_n e^{u-v}\nabla v \\ &= \mu_n e^{u}\nabla \nu \end{aligned} \tag{6}$$

$$\begin{aligned} j_p &= -\mu_p e^{w-u}\nabla w \\ &= -\mu_p e^{-u}\nabla \omega. \end{aligned} \tag{7}$$

Here μ_n and μ_p are the electron and hole mobilities. The variables ν and ω, frequently called Slotboom Variables, are defined by

$$\nu = e^{-v} \tag{8}$$

and

$$\omega = e^{w}. \tag{9}$$

In our case, we use the variables u, ν and ω only for theoretical considerations, whereas u, v and w or u, n, and p are used for the computation.

III. The Discretization of the Continuity Equation

3.1. The Scharfetter-Gummel Method

In 1969, Scharfetter and Gummel (SG) [6] published a robust method for the discretization of the continuity equation in one dimension (1-D). They propose to split the simulation domain into intervals and to assume a constant current within each interval. This current expression is used in the standard central difference scheme to discretize the continuity equation.

In one dimension, and assuming that the current and the mobility are constant over each interval $[x_i\ x_j]$, the current equation

$$j_n = \mu_n e^{u}\frac{dv}{dx} \tag{10}$$

can be integrated and solved

$$j_n = \frac{\mu_n}{x_{ij}}\left(n_j B(u_{ij}) - n_i B(u_{ji})\right). \tag{11}$$

B is the Bernoulli function defined by

$$B(x) \stackrel{\text{def}}{=} \frac{x}{e^x - 1} \tag{12}$$

and

$$u_{ij} \stackrel{\text{def}}{=} u_i - u_j \tag{13}$$

is the difference in the potential between i and j. This form for the current j_n in terms of the nodal values of the potential u_i, u_j are the densities n_i, n_j is used to determine the amount of current flowing out of an interval. The continuity equation for node i can be written as

$$j_n^+ - j_n^- = \frac{R}{2}\left(l^+ + l^-\right) \tag{14}$$

where j_n^+ and j_n^- refer the current in the interval with length l^+ to the right of node i and to the left of node i (with length l^-), respectively. Boundary conditions can be incorporated in the usual way.

3.2. The Box Method

The generalization of the SG approach to higher dimensions led to the well-known Box Method [9], [10], [2]. It can be derived by applying Gauss' Theorem to the current continuity equation (2). The current flow out of a box is approximated by weighted currents along the edges leaving the node that corresponds to the box under consideration. The current along each edge is evaluated using the SG-method according to the assumption that its edge component is constant.

The simulation domain is divided into "boxes" equivalent to the Voronoi elements that correspond to the original grid (Fig. 1). For each of these boxes, the total current flowing in or out is equal to the net generation/recombination within the element. The current flowing through one segment of length d_{ik} in Fig. 1 is approximated under the assumption of a constant tangential component along the edge $\overline{ik}$, leading to a formula for the current completely analogous to the 1-D SG-current (see (11)).

For convenience we consider only the electron current continuity equation (2), (6) and we drop the index n from now on. The case of the hole equation is completely analogous. The current in the direction of an arbitrary unit vector $\boldsymbol{n}$ is given by

$$j \stackrel{\text{def}}{=} \boldsymbol{j}\cdot\boldsymbol{n} = \mu e^{u}\frac{\partial \nu}{\partial n} \tag{15}$$

where

$$\frac{\partial \nu}{\partial n} \stackrel{\text{def}}{=} \nabla \nu \cdot \boldsymbol{n}, \tag{16}$$

is the derivative in the direction of the unit vector $\boldsymbol{n}$. Integrating (15) along $\boldsymbol{n}$ from point i to point k (Fig. 1) leads to

$$j_{ik} = \frac{\mu}{l_{ik}}\left(n_k B(u_{ki}) - n_i B(u_{ik})\right). \tag{17}$$

Here we used

$$l_{ik} \stackrel{\text{def}}{=} l_i - l_k. \tag{18}$$

for the Euclidian distance from point i to point k. j_{ik} is the current flow along the direction of the edge from i to k. μ is the (constant) mobility. u_i and u_k are the electric poten-

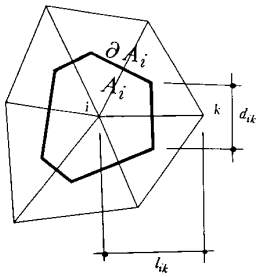

Fig. 1. Box A_i around node i. d_{ik} is the length of the segment perpendicular to the edge $\overline{ik}$ of length l_{ik}.

tials at i and k and n_i, n_k are the densities at the corresponding nodes. The current in (17) determines the current flowing through one particular segment d_{ik} of the box around the particular node i in Fig. 1. Integrating the steady state form of (2) over the box and using Gauss' formula one obtains

$$\int_{A_i} \nabla \cdot \boldsymbol{j}\, dV = \int_{\partial A_i} \boldsymbol{j} \cdot d\boldsymbol{n} = \int_{A_i} R\, dV. \tag{19}$$

The discrete version of the Box Method is given by

$$\sum_k j_{ik} d_{ik} = \mu(A_i) R_i. \tag{20}$$

The sum extends over all neighboring nodes k of node i. The component j_{ik} is the component along edge $\overline{ik}$ and d_{ik} the corresponding measure of the segment of the box A_i perpendicular to $\overline{ik}$. $\mu(A_i)$ is the Euclidian measure of the box A_i and R_i the net recombination/generation rate at node i.

3.3. *Drawbacks of the Box Method*

While the box method has become the standard technique for the discretization of the continuity equations, it suffers from several drawbacks arising from geometrical considerations. Satisfactory results can be obtained only for acute triangulations. Even one obtuse triangle can lead to a large spike in the solution of the equation [7].

In the case of irregular grids, an extension of the SG-based box method will inevitably lead to large problems. As a first fact, it is obvious that the generation of spatial subdivisions with *non-obtuse* elements will be rather difficult [11]. If compared to the 2-D situation, however, it will be no longer possible to improve unsatisfactory grids by methods such as edge-flipping, etc.

During the last few years, several new methods have been proposed to remedy this situation [12]–[17]. Some of them are based on extending the SG-currents evaluated along the edges into the interior of the element. Others use the mixed or even the hybrid finite element method to solve the Continuity Equation.

The basic idea of the next section is to choose the current density in each element in a physically motivated way. We use a local argument to determine the current density uniquely in each element.

IV. Derivation of the Element Current

One can consider (6) or (7) as a system of PDE's in the variables ν or ω. We can view this system in $\boldsymbol{R}^d$, $d = 1$, 2, or 3 for 1-D, 2-D or 3-D, depending on the dimensionality of the problem

$$\nu_{.k} \overset{\text{def}}{=} \frac{\partial \nu}{\partial x_k} = \frac{1}{\mu} e^{-u} j_k, \qquad k = 1, \cdots, d. \tag{21}$$

Again, for the sake of simplicity, we dropped the subscript n to indicate electrons. A necessary condition for a solution ν (in the strong sense) of (21) is (Schwartz's Theorem):

$$\nu_{.ik} = \nu_{.ki} \qquad \text{for } k, i \in \{1, \cdots, d\}. \tag{22}$$

We write the current in vector form

$$\boldsymbol{j} = \mu e^{u} \nabla \nu \tag{23}$$

multiply both sides by e^{-u} and apply the curl operator under the assumption of a constant mobility μ. We get

$$e^{-u}(-\nabla u \times \boldsymbol{j} + \nabla \times \boldsymbol{j}) = \mu \nabla \times \nabla \nu. \tag{24}$$

Because of (22), the right-hand side (RHS) is equal to zero. After dividing the left-hand side (LHS) by the nonzero factor e^{-u} we are left with

$$\nabla \times \boldsymbol{j} = \boldsymbol{j} \times \boldsymbol{E} \tag{25}$$

where we used the expression $\boldsymbol{E} = -\nabla u$ for the electric field. Equation (25) shows that a constant current $\boldsymbol{j}$ implies $\boldsymbol{E} \times \boldsymbol{j} = 0$ and thus

1) either $\boldsymbol{j}$ is parallel to the electric field $\boldsymbol{E}$, or
2) the current $\boldsymbol{j}$ or/and the electric field $\boldsymbol{E}$ is/are zero.

Neither of the two cases is true in general, so that it seems appropriate to take the current $\boldsymbol{j}$ to vary at least linearly to achieve first order accuracy. The most general *Ansatz* for $\boldsymbol{j}$ satisfying (25) can be written as

$$\boldsymbol{j} = \nabla \eta + \eta \boldsymbol{E} \equiv e^{u} \nabla (e^{-u} \eta) \tag{26}$$

where η is some function, given in terms of the linear (in the case of simplexes), bilinear (in the case of quadrilaterals) or trilinear (in the case of bricks) basis functions ϕ_i and the nodal values η_i

$$\eta = \sum_i \eta_i \phi_i. \tag{27}$$

We choose as basis functions the usual *hat functions*, which are one at one node and zero at every other node and linear in between.

Using the (26) and (6), we have under the assumption of constant mobility μ

$$e^{-u} \boldsymbol{j} = \nabla (e^{-u} \eta) \tag{28}$$

$$e^{-u} \boldsymbol{j} = \nabla (\mu \nu) \tag{29}$$

and, after taking the difference

$$\nabla (e^{-u} \eta - \mu e^{-\nu}) = 0 \tag{30}$$

where we used the quasi-Fermi variable v instead of the Slotboom variable $\nu \overset{\text{def}}{=} e^{-v}$.

Equation (30) implies

$$\eta = \mu(n + \alpha e^{u}) \tag{31}$$

where α is some integration constant and n is the density. In Appendix A, we shall discuss the uniqueness of the Ansatz in (26) and (31).

To determine α, assume that in a particular element Ω_e

$$\int_{\Omega_e} \nabla \cdot \boldsymbol{j}\, d\Omega = 0. \tag{32}$$

Together with (26) and (27), this leads to

$$\int_{\Omega_e} \nabla\eta \cdot \boldsymbol{E}\, d\Omega = 0. \tag{33}$$

Remark that the electric field $\boldsymbol{E}$ is according to 27 piecewise constant. We write the function η in terms of the basis functions ϕ_k (eq. (27), put this into (33), integrate over one element T and obtain

$$\sum_i (n_i + \alpha e^{u_i}) E_i = 0 \tag{34}$$

where we used

$$E_i \overset{\text{def}}{=} \int_{\Omega_e} \nabla\phi_i \cdot \boldsymbol{E}\, d\Omega \equiv -\sum_j u_j a_{ji} \tag{35}$$

and

$$a_{ji} \overset{\text{def}}{=} \int_{\Omega_e} \nabla\phi_j \cdot \nabla\phi_i\, d\Omega \tag{36}$$

is the element stiffness matrix for Ω_e of the Laplacian operator. Equation (34) completely determines α. It is given by

$$\alpha = -\frac{\sum_k n_k E_k}{\sum_k e^{u_k} E_k} \tag{37}$$

and, therefore, the value of η at node i is given by

$$\eta_i = \mu\left(n_i - \frac{\sum_k n_k E_k}{\sum_k e^{u_k} E_k} e^{u_i}\right). \tag{38}$$

The current in each element is now uniquely defined to be

$$\boldsymbol{j} = \sum_i \mu\left(n_i - \frac{\sum_k n_k E_k}{\sum_k e^{u_k} E_k} e^{u_i}\right)(\nabla\phi_i + \phi_i \boldsymbol{E}) \tag{39}$$

where the sum over i runs through the element basis functions ϕ_i.

In Appendixes B and C, we shall discuss the limiting cases of the above current expression for pure drift and pure diffusion. Appendix D deals with the equivalence of our new sheme with the original Scharfetter–Gummel expression [6].

In the derivation of α above, we completely neglected the case of a vanishing denominator. We will treat this singular case in some detail in Appendix E.

V. The Weak Formulation

5.1. Preliminaries

Let d denote the number of space dimensions, Ω be an open region in $\boldsymbol{R}^d$ with piecewise smooth boundary Γ, and $\boldsymbol{n}$ be the unit outward normal vector to Γ. We assume that Γ is the closure of the union of the two disjoint subsets Γ_g, Γ_h. Consider a discretization of Ω into elements Ω_e. Each Ω_e is taken to be an open set with boundary $\Gamma_e \overset{\text{def}}{=} \partial\Omega_e$ (see Fig. 2):

Assume that

$$\bar{\Omega} = \bigcup_e \bar{\Omega}_e \tag{40}$$

$$\Gamma \subset \bigcup_e \Gamma_e. \tag{41}$$

The interfaces are defined to be

$$\Gamma_{\text{int}} \overset{\text{def}}{=} \bigcup_e \Gamma_e \backslash \Gamma. \tag{42}$$

As a weighting function space, we use the piecewise linear (bilinear, trilinear) basis functions ϕ_i for simplexes (quadrilaterals, bricks), satisfying

$$\phi_i(k) = \delta_{ik} \tag{43}$$

where k stands for node k and δ_{ik} is the Kronecker delta defined by

$$\delta_{ik} \overset{\text{def}}{=} \begin{cases} 1, & \text{if } i = k \\ 0, & \text{if } i \neq k. \end{cases} \tag{44}$$

Note that for this set of element basis functions in (43)

$$\sum_i \phi_i = 1 \tag{45}$$

which implies

$$\sum_i \nabla\phi_i = 0. \tag{46}$$

5.2. The Continuity Equation and the Weighted Residual Formulation

The goal is to find a function ν satisfying

$$\nabla \cdot \boldsymbol{j} = R \text{ in } \Omega \tag{47}$$

and also certain boundary conditions. We shall require that

$$\nu = g \text{ on } \Gamma_g \tag{48}$$

and

$$j \overset{\text{def}}{=} \boldsymbol{n} \cdot \boldsymbol{j} = -h \text{ on } \Gamma_h. \tag{49}$$

Let the current $\boldsymbol{j}$ be given by (6). Then (47) describes a highly nonlinear convection–diffusion problem.

Let $\boldsymbol{x}$ be an arbitrary point on Γ_{int} in Fig. 2. We arbitrarly designate one side of Γ_{int} to be the *plus side* and the other be the *minus side* with corresponding unit normal

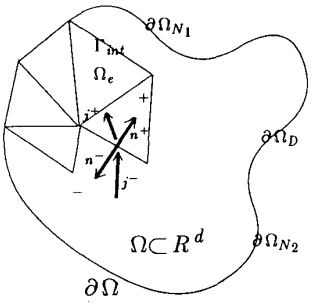

Fig. 2. Simulation domain Ω is divided into finite elements Ω_e. The union of $\partial\Omega_e$ not lying on $\partial\Omega$ is Γ_{int}. Notice the convention for $\boldsymbol{n}^+$ and $\boldsymbol{n}^-$ on an interface.

vectors $\boldsymbol{n}^+$ and $\boldsymbol{n}^-$ pointing in the plus and minus direction, respectively.

The jump in the flow of $\boldsymbol{j}$ across Γ_{int} is defined by [18]

$$[j] \stackrel{\text{def}}{=} \boldsymbol{j}^+ \cdot \boldsymbol{n}^+ + \boldsymbol{j}^- \cdot \boldsymbol{n}^- \tag{50}$$

where we used $\boldsymbol{j}^+$ and $\boldsymbol{j}^-$ to indicate the current on the plus and minus side, respectively. Note that the jump is invariant with respect to reversing *plus* and *minus*.

Throughout, we shall assume that the trial solution v satisfies (48) and the weighting function ϕ satisfies

$$\phi = 0 \text{ on } \Gamma_g. \tag{51}$$

The variational formulation for (47) subject to the boundary conditions in (48) and (49) is given by

$$-\int_\Omega \phi R \, d\Omega - \int_\Omega \nabla\phi \cdot \boldsymbol{j} \, d\Omega + \int_{\Gamma_h} \phi h \, d\Gamma = 0, \qquad \forall\phi. \tag{52}$$

In this equation, the ϕs belonging to the specified test function space satisfying (48). Using integration by parts in each element Ω_e, (52) can be written as [18]

$$\sum_e \int_{\Omega_e} \phi(\nabla \cdot \boldsymbol{j} - R) \, d\Omega + \int_{\Gamma_h} \phi(j + h) \, d\Gamma + \int_{\Gamma_{\text{int}}} \phi[j] \, d\Gamma = 0, \qquad \forall\phi. \tag{53}$$

from which we see that the corresponding Euler–Lagrange equations are (47) restricted to the element interiors Ω_e, (49) and the total-flux continuity condition across interelement boundaries, i.e.,

$$[j] = 0 \text{ on } \Gamma_{\text{int}}. \tag{54}$$

5.3. The Finite Element Formulation for Simplices

We use for our discretization n-dimensional simplexes, i.e., intervals, triangles or tetrahedras for $n = 1, 2, 3$. Basis functions are the standard piecewise-linear functions satisfying

$$\phi_i(x_j) = \delta_{ij} \tag{55}$$

where x_j are the coordinates of node j and δ_{ij} is the Kronecker delta defined above. Note that for this set of element basis functions, (45) and (46) hold. Neglecting the contribution due to Neumann boundary condictions, the contribution of element Ω_e to the kth equation of the discretized version of the current continuity equation ((52)) is

$$F_k^{\Omega_e} = o - \int_{\Omega_e} \phi_k R \, d\Omega - \sum_l \mu_n \left(n_l - \frac{\sum_j n_j E_j}{\sum_j e^{u_{jl}} E_j} \right) \cdot \left(a_{kl} + \frac{E_k}{n+1} \right) = 0 \tag{56}$$

where a_{kl} and E_k are defined by (36) and (35), respectively. The sum over l in the second term of (56) extends over the nodes of the element with this choice of basis functions in (55).

VI. Incorporation of Magnetic Field Effects

6.1. Introduction

In the presence of a magnetic field $\boldsymbol{B}$ Poisson's equation (1) and the continuity equations for both the electrons and holes, (2) and (3), remain the same. Instead of (6) and (7), we have for the electron and hole current [19]

$$\boldsymbol{j}_k^B = \left(\boldsymbol{j}_k^0 - \mu_k^* \boldsymbol{j}_k^0 \times \boldsymbol{B} + (\mu_k^*)^2 (\boldsymbol{j}_k^0 \cdot \boldsymbol{B}) \boldsymbol{B} \right) / \left(1 + (\mu_k^* B)^2 \right) \tag{57}$$

where we use k for n (electron current) and p (hole current) respectively, $B = |\boldsymbol{B}|$ and μ_k^* is the Hall mobility in the presence of the magnetic field $\boldsymbol{B}$

$$\mu_k^* \stackrel{\text{def}}{=} \begin{cases} r_n \mu_n, & \text{if } k = n \\ -r_p \mu_p, & \text{if } k = p. \end{cases} \tag{58}$$

and the Hall scattering factor r_k, $k = n, p$ is on the order of unity. Note that $\mu_n^* > 0$ and $\mu_p^* < 0$. $\boldsymbol{j}_k^0$ is the current due to the electric field $\boldsymbol{E}$ and the diffusion only. It is given by

$$\begin{aligned} \boldsymbol{j}_n^0 &= -\mu_n e^{u-v} \nabla v \\ \boldsymbol{j}_p^0 &= -\mu_p e^{w-u} \nabla w. \end{aligned} \tag{59}$$

The boundary conditions for the Continuity Equations are

$$j_n \stackrel{\text{def}}{=} \boldsymbol{j}_n \cdot \boldsymbol{n} = g_n \text{ on } \Gamma_h \tag{60}$$

$$j_p \stackrel{\text{def}}{=} \boldsymbol{j}_p \cdot \boldsymbol{n} = g_p \text{ on } \Gamma_h$$

$$v = g_n \text{ on } \Gamma_g \tag{61}$$

$$w = g_p \text{ on } \Gamma_g$$

where $\boldsymbol{n}$ is again the outward unit normal, and

$$\partial\Omega = \Gamma_h \cup \Gamma_g \tag{62}$$

$$\Gamma_h \cap \Gamma_g = \varnothing. \tag{63}$$

The Dirichlet boundary condition for Poisson's equation (1) is given by

$$u = g_u \text{ on } \Gamma_g. \tag{64}$$

The harder part of the problem is to determine the Neumann boundary condition on Γ_h. If we just consider the majority carriers, e.g., the electrons in the vicinity of the boundary Γ_h, j_n^0 is very well approximated by [20], [21]

$$j_n^0 = \mu_n e^{u-v} E. \tag{65}$$

In the case of homogeneous Neumann boundary conditions setting j_n in (60) to zero leads to the equation

$$E_n = -\mu_n^* B E_t \tag{66}$$

where the subscripts n and t in E denote to normal and tangential components of the electric field. With

$$-\frac{\partial u}{\partial n} \stackrel{\text{def}}{=} E_n = -\mu_n^* B E_t \text{ on } \Gamma_h \tag{67}$$

leads to an oblique boundary condition for the Poisson equation. Some authors [22] overcome this difficulty by surrounding the device with a field oxide region (assuming zero trapped charge density) and solving Poisson's equation over the entire domain. At the open boundaries of the oxide, homogeneous Neumann boundary conditions are imposed. The semiconductor/oxide interface is assumed ideal. Others [23] use

$$\frac{\partial^2}{\partial x^2}(p - n - N) = 0 \tag{68}$$

which is weaker than the conditions commonly used on floating boundaries.

6.2. Example: 2-D Finite Element Formulation in the Case of a Magnetic Field

In this case the magnetic field $\boldsymbol{B}$ is perpendicular to the simulation domain. Thus the last term in (57) is zero and the current is given by

$$\boldsymbol{j}_k^B = \frac{(\boldsymbol{j}_k^0 - \mu_k^* \boldsymbol{j}_k^0 \times \boldsymbol{B})}{\left(1 + (\mu_k^* \boldsymbol{B})^2\right)}. \tag{69}$$

For the current $\boldsymbol{j}_k^0$ we use the *Ansatz* of (26). In order to determine α in (31) we assume that within an element Ω_e

$$\int_{\Omega_e} \nabla \cdot \boldsymbol{j}_k^B \, d\Omega = 0. \tag{70}$$

One should note that this is completely analogous to the condition in (32). Using (69), (39), and some vector algebra we obtain

$$\int_{\Omega_e} \nabla\eta \cdot (\boldsymbol{E} + \mu_k^* \boldsymbol{E} \times \boldsymbol{B}) \, d\Omega = 0 \tag{71}$$

from which we find α

$$\alpha = -\frac{\sum_i n_i \bar{E}_i}{\sum_i e^{u_i} \bar{E}_i} \tag{72}$$

with

$$\bar{E}_i \stackrel{\text{def}}{=} \int_T \nabla\phi_i \cdot (\boldsymbol{E} + \mu_k^* \boldsymbol{E} \times \boldsymbol{B}) \, d\Omega. \tag{73}$$

From (72) it is straightforward to determine the finite element formulation in the case of a nonzero magnetic field $\boldsymbol{B}$. For the electron current continuity equation we have

$$\int_{\Omega_e} \boldsymbol{j}_n^B \cdot \nabla\phi_k \, d\Omega = \bar{\mu}_n \sum_i (n_i + \alpha e^{u_i}) \left(a_{ik} + \frac{\bar{E}_k}{d+1} + \beta \tilde{a}_{ik} \right) \tag{74}$$

with the definitions

$$\alpha_n \stackrel{\text{def}}{=} -\frac{\sum_l n_l \bar{E}_l}{\sum_l e^{u_l} \bar{E}_l} \tag{75}$$

$$\bar{\mu}_n \stackrel{\text{def}}{=} \frac{\mu_n}{1 + \beta_n^2} \tag{76}$$

$$\bar{E}_l \stackrel{\text{def}}{=} E_l + \beta_n \tilde{E}_l \tag{77}$$

$$\beta_n \stackrel{\text{def}}{=} \mu_n^* B \tag{78}$$

$$\tilde{E}_l \stackrel{\text{def}}{=} \int_{\Omega_e} (\boldsymbol{E} \times \nabla\phi_i)_z \, d\Omega \tag{79}$$

$$\tilde{a}_{ik} \stackrel{\text{def}}{=} \int_{\Omega_e} (\nabla\phi_i \times \nabla\phi_k)_z \, d\Omega. \tag{80}$$

a_{ik} and E_i are defined in (36) and (35).

The terms including the recombination/generation or boundary conditions in (33) are assumed to be the same in the case of a nonzero magnetic field.

VII. Results

7.1. The Mock Diode

As a first example we took a one-dimensional diode with known analytical solution [24] and extended it to the multi-dimensional case. In the low injection level, the applied voltage in forward direction is 20 and in the high injection level 28 in normalized units. The corresponding doping concentration is shown in Fig. 3. The Gauss–Seidel method was used to solve the coupled system of equations. Various 2-D and 3-D grids as shown in Figs. 4 and 7 were used in the simulation. In Figs. 5 and 6, we compare the relative error in the electron current as obtained by the new discretization scheme and the box method with the analytical solution for both injection levels using a 2-D grid for the calculation.

Fig. 7 defines the grid quality parameter δ for a 3-D grid, and Fig. 8 shows the corresponding relative error of the electron current in the low and high injection levels.

7.2. A Magnetic Field Sensor

As a second example, we studied the effect of a constant magnetic field, perpendicular to the simulation do-

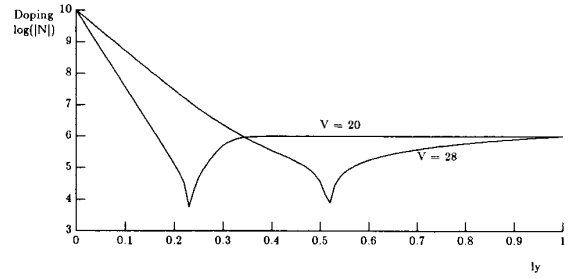

Fig. 3. Doping concentration (cm^{-3}) versus distance (arbitrary units).

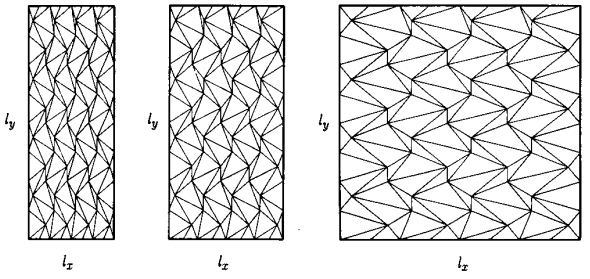

Fig. 4. 2-D-grids with $l_x/l_y = 0.375, 0.5, 1.0$.

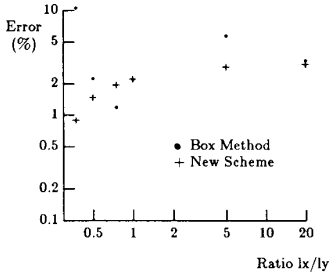

Fig. 5. Relative error of the electron current in the low injection level ($u = 20$) versus the ration l_x/l_y.

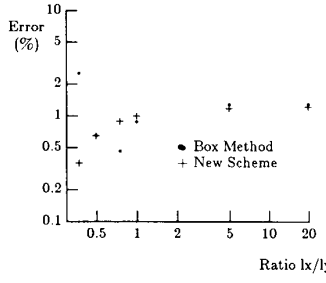

Fig. 6. Relative error of electron current in the high injection level ($u = 28$) versus the ration l_x/l_y.

main in a homogeneous Hall sensor. The dimensions, doping concentration and the applied voltage are the same as in [20]. For the computation we used the grids shown in Fig. 4. Fig. 9 shows the effect of an applied magnetic field $B_z = -2.0$ T under an applied bias of 0.1 Volts. The obtained results are in very good agreement with the results presented by them.

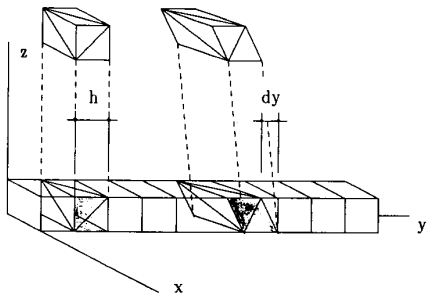

Fig. 7. 3-D-grid and definition of grid quality parameter γ. The tetrahedra on the left is an undistorted one, whereas on the right you see the analogous, but distorted. $l_x = 0.1$, $l_y = 1.0$, $l_z = 0.1$. γ is defined by dx/h.

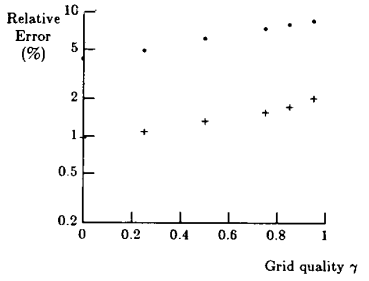

Fig. 8. Relative error of the electron current in the low and high injection level versus grid quality parameter γ.

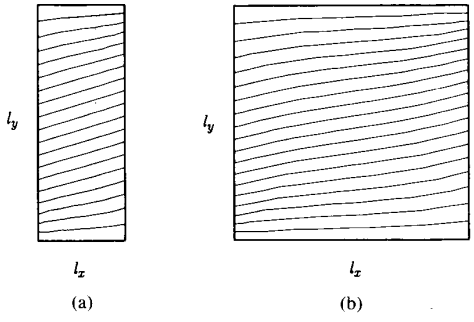

Fig. 9. Effect of a magnetic field $B_z = -2.0$ T on the equipotential lines in homogeneously doped n-type silicon Hall plates (10^{16} cm^{-3}) for l_x/l_y-ratios of 0.375 (a) and 1.0 (b). The applied bias is 0.1 V.

VIII. Conclusion

We presented a new approach to discretize the current continuity equations. The assumptions we used—the linearity of the current and a constant mobility within each element and the zero divergence—are not restrictive, but nonetheless necessary in order to model the current accurately. In some sense the method is similar to the hybrid finite element method first introduced by Pian [25], where he eliminates the local variables by static condensation. We, on the other hand, use the integrability condition (25), and the assumption concerning the divergence of the current (32), to eliminate the local variables, determining the coefficients of the linear Ansatz of the current.

The weak formulation of the current continuity equation is the same as in the hybrid finite element method. It assures that the current continuity equation is satisfied in a weak sense together with the boundary conditions and current flux continuity across interelement boundaries. We derived the equations including the effect of a magnetic field, and gave formulas for the 2-D case in some detail.

A comparison of the Box Method with the proposed method is given. We simulated a n^+ p-diode, for which we know the exact analytical solution and we have shown that the proposed method is superior to the Box Method in cases of nonacute triangulations. We also presented some results concerning the effect of magnetic fields.

The Appendix was devoted to the study of some limiting cases and to the obtuse angle problem. We have shown that the new method reduces to the expected limits in the pure diffusion, pure drift and in the 1-D case. The obtuse angle problem was shown not to be a serious drawback.

Appendix

A. Uniqueness of the Current Ansatz

The discretization presented above consists of the construction of a low order polynominal approximation to the elemental current, $\boldsymbol{j}$. The current is constrained to satisfy the curl condition, (25), the edge condition, (30) and the divergence condition, (32). To this end, the current is written as (26):

$$\boldsymbol{j} = \nabla\eta + \eta\boldsymbol{E} \tag{81}$$

where the function η is chosen to satisfy both the edge condition and the divergence condition.

We note that the function η is not unique but is determined only to within a solution which produces zero current. That is, the current, $\boldsymbol{j}$, is invariant under the transformation

$$\eta \rightarrow \eta' = \eta + Ae^{u} \tag{82}$$

where A is an arbitrary constant. Without any loss of generality, this constant may be set equal to zero. This transformation can be viewed as a gauge transformation in the theory of Maxwell's equations ([26, chap. 5.4]).

B. The Case of Pure Drift

Without loss of generality, we will consider only the continuity equation for the electrons. The case of the hole current is completely analogously. By n we denote the constant electron density. The electron current is given by

$$\boldsymbol{j}_n = -\mu_n n\nabla v. \tag{83}$$

For a constant electron density n, we have $u \equiv v$ and, therefore,

$$\boldsymbol{j}_n = -\mu_n n\nabla u. \tag{84}$$

Using the constant electron density n and the expression for η we have

$$\eta_i = \mu_n\left(1 - \frac{\sum\limits_k E_k}{\sum\limits_k e_k E_k}\, e_i\right). \tag{85}$$

where

$$e_i \equiv e^{u_i}. \tag{86}$$

The second term on the right-hand side in (85) is zero, as can be seen from

$$\sum_k E_k = -\sum_k \sum_l u_l a_{kl}^T = -\sum_l u_l \sum_l a_{kl}^T \tag{87}$$

and the fact that

$$\sum_l a_{kl}^{\Omega_e} = \sum_l \int_T \nabla\phi_k \cdot \nabla\phi_l \, dV = \int_T \nabla\phi_k \cdot \sum_l \nabla\phi_l \equiv 0, \tag{88}$$

because the last sum in (88) is zero for the piecewise-linear (bilinear, trilinear) basis functions ϕ_l. Thus η is constant in an element

$$\eta = \mu_n n. \tag{89}$$

We finally end up with the finite element formulation

$$\int_\Omega \phi R \, d\Omega = \mu_n n \sum_e \int_{\Omega_e} \nabla\phi \cdot \nabla u \, d\Omega + \int_{\Gamma_h} \phi h \, d\Gamma, \qquad \forall\phi \tag{90}$$

which is exactly the finite element formulation for a Poisson Equation of the form

$$-\mu_n n\Delta u = R \text{ in } \Omega \tag{91}$$

with boundary conditions on the Neumann part

$$\nabla u \cdot \boldsymbol{n} = h \text{ on } \Gamma_h \tag{92}$$

and on the Dirichlet part of the boundary $\partial\Omega$

$$u = g \text{ on } \Gamma_g. \tag{93}$$

C. The Case of Pure Diffusion

In this case the electric field $\boldsymbol{E}$ is zero. For convenience, let us again consider the electron continuity equation only. The electron current is then given by

$$\boldsymbol{j}_n = \nabla\eta. \tag{94}$$

η, expressed in terms of basis functions ϕ_i is given by

$$\eta = \sum_i \eta_i \phi_i. \tag{95}$$

Using the expression of η in terms of the electron density n, the integration constant α and the electric potential u the electron current can be written as

$$\boldsymbol{j}_n = \mu_n \sum_i (n_i + \alpha e^{u_i})\nabla\phi_i. \tag{96}$$

Note, that because of the constant potential u the second term in the sum is zero independent of the value of α, so that

$$\boldsymbol{j}_n = \mu_n \sum_i n_i \nabla\phi_i = \mu_n \nabla n \tag{97}$$

is the electron current defined in an element. The finite element formulation reads

$$\int_\Omega \phi R \, d\Omega = -\mu_n \sum_e \int_{\Omega_e} \nabla\phi \cdot \nabla n \, d\Omega + \int_{\Gamma_h} \phi h \, d\Gamma, \qquad \forall\phi. \tag{98}$$

This is again the finite element formulation of an equation of the form

$$\mu_n \Delta n = R \text{ in } \Omega \tag{99}$$

with boundary conditions on the Neumann part

$$\nabla n = h \text{ on } \Gamma_h \tag{100}$$

and the Dirichlet part of the boundary $\partial\Omega$

$$n = g \text{ on } \Gamma_g. \tag{101}$$

D. Recovering the Scharfetter and Gummel Method in 1-D

In the 1-D case we consider an interval $[x_1, x_2] \subset \boldsymbol{R}^1$. As in the cases of pure drift and pure diffusion we will only look at the electron current continuity equation. We use as basis functions the standard piecewise linear *hat functions*

$$\phi_2(x) \overset{\text{def}}{=} \frac{x - x_1}{x_2 - x_1}, \quad \phi_1(x) \overset{\text{def}}{=} 1 - \phi_1(x). \tag{102}$$

The case of the hole equation can be treated completely identical. The following identities can then be derived easily:

$$\frac{d\phi_1}{dx} \equiv -\frac{d\phi_2}{dx} \equiv -\frac{1}{x_{21}} \tag{103}$$

$$a_{12} \equiv -a_{11} \equiv -a_{22} \equiv -\frac{1}{x_{21}} \tag{104}$$

or in general,

$$a_{ik} = (-1)^{i+k} \frac{1}{x_{21}} \tag{105}$$

$$E_k = -(-1)^k \frac{u_{21}}{x_{21}}. \tag{106}$$

The contribution of this interval $[x_1, x_2]$ to the kth discretized, stationary current continuity equation (56) is

$$F_k^{[x_1,x_2]} = \int_{x_1}^{x_2} j_n \frac{d\phi_k}{dx} \, dx - \int_{x_1}^{x_2} \phi_k R \, dx = 0 \tag{107}$$

and with the appropriate order of integration in the second term of (107)

$$F_k^{[x_1,x_2]} = \mu_n \sum_{i=1}^{2} (n_i + \alpha e_i)\left(a_{ik} + \frac{E_k}{2}\right) - R_k \frac{x_{21}}{2} = 0. \tag{108}$$

With

$$\alpha = -\frac{n_{12}}{e_1 - e_2} \tag{109}$$

in (108) we obtain after some algebra

$$F_k^{[x_1,x_2]} = \frac{\mu_n(-1)^k}{x_{21}} \sum_{i=1}^{2} \left(n_i - \frac{n_{21}}{e_{21}} e_i\right)\left((-1)^i - \frac{u_{21}}{2}\right) - R_k \frac{x_{21}}{2} = 0 \tag{110}$$

and finally,

$$F_k^{[x_1,x_2]} = \frac{\mu_n(-1)^k}{x_{21}} \left(n_2 B(u_{21}) - n_1 B(u_{12})\right) - R_k \frac{x_{21}}{2} = 0, \qquad k = 1, 2. \tag{111}$$

Here, $B(x)$ is the well known Bernoulli function, R_k the recombination/generation rate at node k and x_{21} is the length of the interval $x_2 - x_1$. Note that (111) is exactly the Scharfetter and Gummel discretization formula in 1-D [6].

E. The Obtuse Angle Problem

We want to consider the problem of the vanishing denominator in the expression for α in (37). We will restrict to the 2-D case. In 3-D the problem is analogous. In 1-D the terms including the eventually vanishing denominator cancel exactly and the nice Bernoulli functions appears.

The assumption (32) for the divergence of the current within an element Ω_e leads in the case of a linear, bilinear or trilinear function η to the condition

$$\nabla\eta \cdot \boldsymbol{E} = 0 \tag{112}$$

which essentially says that $\nabla\eta$ is to be perpendicular to the electric field $\boldsymbol{E}$. Note also, that the component of the current

$$\boldsymbol{j} = \nabla\eta + \eta\boldsymbol{E} \tag{113}$$

perpendicular to $\boldsymbol{E}$ is constant, whereas the component in the direction of $\boldsymbol{E}$ varys linearly. This leads to the condition that in the equation

$$0 = \nabla \cdot \boldsymbol{j} = \mu \sum_i (n_i + \alpha e_i)\nabla\phi_i \cdot \boldsymbol{E} \tag{114}$$

α is not determined whenever

$$\sum_i e_i \nabla\phi_i \cdot \boldsymbol{E} = 0. \tag{115}$$

In the following we will show, that (115) defines a circle, such that if a vertex of the triangle lies on this circle the factor in front of α in (113) vanishes. To this end we will consider a normalized triangle.

By a suitable linear transformation of the coordinates, and eventually permuting the node numbers, we can transform any triangle in the normalized form shown in Fig. 10. Denoting the coordinates of vertex 2 by (x, y)

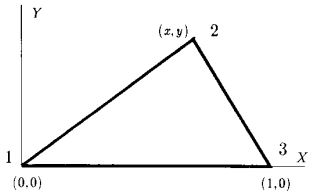

Fig. 10. Normalized triangle with node 2 having coordinates (x, y), such that $x > 0$ and $0 < y < 1$.

we write the denominator of (115) in terms of (x, y)

$$f(x, y) \stackrel{\text{def}}{=} \sum_i e_i \nabla \phi_i \cdot \boldsymbol{E} \tag{116}$$

It can be shown, that the values (x, y) satisfying

$$f(x, y) = 0 \tag{117}$$

lie on the circle, called *obtuse circle*, defined by

$$y^2 + \left(x - \frac{e_r + u_r}{2}\right)^2 - \left(\frac{e_r - u_r}{2}\right)^2 = 0 \tag{118}$$

where we used

$$u_r \stackrel{\text{def}}{=} \frac{u_{21}}{u_{31}}, \quad e_r \stackrel{\text{def}}{=} \frac{e_2 - e_1}{e_3 - e_1}. \tag{119}$$

Given $0 < \epsilon << 1$ we define

$$u_{31} \stackrel{\text{def}}{=} -\frac{\ln \epsilon}{\epsilon}, \quad u_{21} \stackrel{\text{def}}{=} (1 - \epsilon) u_{31}. \tag{120}$$

It is easy to see, that

$$u_r = 1 - \epsilon, \quad e_r \to e^{u_{21} - u_{31}} = \epsilon \tag{121}$$

in which case the center and the radius of the obtuse circle are given by

$$(x_M, y_M) \equiv \left(\frac{u_r + e_r}{2}, 0\right) = \left(\frac{1}{2}, 0\right) \tag{122}$$

$$R \equiv \frac{u_r - e_r}{2} = \frac{1}{2} - \epsilon \tag{123}$$

respectively.

We have shown that for any obtuse triangle, an electric potential u can be chosen, such that the denominator of α vanishes. We will now show, that the gradient of $f(x, y)$ in (116) is rather large in the limit of large u_{21} and that in this case the singularity in α is very steep and well localized.

The gradient at $f(x, y) = 0$ is given by

$$\nabla f = 2(e_3 - e_1) u_{31} \left(y^{-1}, y^{-2}\left(x - \frac{e_r + u_r}{2}\right)\right)^T. \tag{124}$$

As an example, we calculate $df = |\nabla f(f \equiv 0)|\, dl$ for the case of $dl = 10^{-9}$, $y = 0.1$, $u_{31} = 1.0$. In order to have $df \approx 10^{-15}$, the increment dl we have to move is on the order of 10^{-14}. It is therefore satisfactory, to limit the smallest value of the denominator to the machine epsilon. This in turn corresponds to the inaccuracy of the coordinates of the nodes of the triangle.

There is also a physical reasoning: assume a very small magnetic field, applied just to this element. Because of (72) and (75), the denominator can be made positive, say greater than the machine epsilon. Again the magnetic field, which has to be applied in order to achieve this, is very small.

Note that for small u_{21} and u_{31} the radius of the obtuse circle tends to zero and the center to $(x_M, y_M) = (u_{21}/u_{31}, 0)$. This shows, that the obtuse angle problem is also not serious in the case of a small electric field.

F. Assembly of the Right-Hand Side (RHS) and the Matrix

Up to now, we have not mentioned how to evaluate the RHS and the matrix in the most accurate way. As is already known for the evaluation of the Bernoulli functions, an acurate evaluation is absolutely necessary to obtain physically meaningful results. In our calculations we found that under conditions of medium to high current flow, the new method is rather insensitive to the evaluation of the matrix and the right-hand side. In the reverse biased case, one has to be very careful. The best way is to assemble over edges, and not over vertices. This means for example, that the double sum

$$\sum_i \sum_j e_i u_j a_{ij} \tag{125}$$

has to be evaluated as

$$\sum_i \sum_{j<i} (e_i - e_j) u_{ij} a_{ij} \tag{126}$$

in order to obtain the most accuracy.

We found that the potential drop across an element should not be larger than 0.25 V for a 32-bit machine and 0.5 V for a 64-bit machine. This is a reasonable value, also for other aspects such as the discretization of the Poisson's Equation. It has been shown [27] that a not accurately resolved electric potential causes large errors in the terminal currents.

REFERENCES

[1] H. K. Gummel, "A self-consistent iterative scheme for one-dimensional steady-state transistor calculations," *IEEE Trans. Electron Devices*, vol. ED-11, pp. 455-465, 1969.

[2] R. E. Bank, D. J. Rose, and W. Fichtner, "Numerical methods for semiconductor device simulation," *IEEE Trans. Electron Devices*, vol. ED-30, pp. 1031-1041, 1983.

[3] R. E. Bank, J. W. M. Coughran, W. Fichtner, E. H. Grosse, D. J. Rose, and R. K. Smith, "Transient simulation of silicon devices and circuits," *IEEE Trans. Electron Devices*, vol. ED-32, pp. 1992-2007, 1985.

[4] J. W. M. Coughran, M. R. Pinto, and R. K. Smith, "Computation of steady-state CMOS latchup characteristics," *IEEE Trans. Computer-Aided Design*, to be published.

[5] M. S. Mock, "Quadrilateral elements and the Scharfetter-Gummel method," in *Proc. Int. Conf. on Simulation of Semiconductor Devices and Processes*, (K. Board and D. R. J. Owen, Eds.), University College of Swansea, Swansea, U. K., pp. 298-309, Swansea, U. K., 1984.

[6] D. L. Scharfetter and H. K. Gummel, "Large-signal analysis of a silicon Read diode oscillator," *IEEE Trans. Electron Devices*, vol. ED-16, pp. 64-77, 1969.
[7] M. R. Pinto, C. S. Rafferty, and R. W. Dutton, "PISCES II: Poisson and continuity equation solver," Stanford Univ., Stanford, CA 94305, 1984.
[8] S. Selberherr, A. Schütz, and H. W. Pötzl, "MINIMOS—A two-dimensional MOS transistor analyzer," *IEEE Trans. Electron Devices*, vol. ED-27, pp. 1540-1550, 1980.
[9] R. S. Varga, *Matrix Iterative Analysis*. Englewood Cliffs: Prentice-Hall, 1962.
[10] E. M. Buturla, P. E. Cottrell, B. M. Grossman, and A. K. Salsburg, "Finite-element analysis of semiconductor devices: The FIELDAY program," *IBM J. Res. Develop.*, vol. 25, pp. 218-239, 1981.
[11] P. Conti and W. Fichtner, "Automatic grid generation for 3d device simulation," in *Proc. Third Int. Conf. on Simulation of Semiconductor Devices and Processes*, (G. Baccarani and M. Rudan, Eds.), 1988.
[12] P. Markowich, *The Stationary Semiconductor Device Equations*. New York: Springer-Verlag, 1985.
[13] R. R. O'Brien, G. R. Srinivasan, and N. A. Azziz, "Some questions relating to process modeling and device analysis," in *Proc. Int. Conf. on Simulation of Semi-cunductor Devices and Processes*, (K. Board and D. R. J. Owen, Eds.), University College of Swansea, Swansea, U. K., pp. 454-459, Swansea, U. K., 1986.
[14] P. J. Mole, "Discretization of the semiconductor current continuity equation for finite element solvers in 2 and 3 dimensions," in *Proc. Fourth Conf. Numerical Analysis of Semiconductor Devices and Integrated Circuits—NASECODE IV*, (J. J. H. Miller, Ed.), Trinity College, Dublin, Ireland, pp. 429-435, Boole Press, 1985.
[15] M. S. Towers and D. Gunasekera, "An exponentially-fitted element to give piecewise bilinear current density distribution in the discretized semiconductor current continuity equations," in *Proc. Fourth Conf. Numerical Analysis of Semiconductor Devices and Integrated Circuits—NASECODE IV*, (J. J. H. Miller, Ed.), Trinity College, Dublin, Ireland, pp. 525-529, Boole Press, 1985.
[16] J. S. V. Welij, "Basis functions matching tangential components on element edges," in *Proc. Int. Conf. Simulation of Semiconductor Devices and Processes*, (K. Board and D. R. J. Owen, eds.), (Univ. College of Swansea, Swansea, U. K.), pp. 371-383, Pineridge Press, Swansea, U. K., 1986.
[17] W. H. A. Schilders, S. J. Polak, and J. S. V. Welij, "Solution of semiconductor device problems, using arbitrary quadrilateral grids," in *Proc. Fifth Conf. Numerical Analysis of Semiconductor Devices and Integrated Circuits—NASECODE V*, (J. J. H. Miller, Ed.), Trinity College, Dublin, Ireland, pp. 313-320, Boole Press, 1987.
[18] T. J. R. Hughes and A. Brooks, "A theoretical framework for petrov-galerkin methods with discontinuous weighting functions: application to the streamline-upwind procedure," in *Finite Elements in Fluids*, (R. G. Gallagher, D. H. Norrie, J. T. Oden, and O. C. Zienkiewicz, Eds.). Wiley, 1982.
[19] H. P. Baltes and R. S. Popovíc, "Integrated semiconductor magnetic field sensors," *Proc. IEEE*, vol. 74, pp. 1107-1132, 1986.
[20] H. P. Baltes, L. Andor, A. Nathan, and H. G. Schmidt-Weinmar, "Two-dimensional numerical analysis of a silicon magnetic field sensor," *IEEE Trans. Electron Devices*, vol. ED-31, pp. 996-999, 1984.
[21] R. S. Popovíc and R. Widmer, "Magnetotransistors in cmos technology," *IEEE Trans. Electron Devices*, vol. ED-33, pp. 1334-1340, 1986.
[22] W. Allegretto, A. Nathan, and H. P. Baltes, "Two-dimensional numerical analysis of silicon bipolar magnetotransistors," in *Proc. Fifth Conf. Numerical Analysis of Semiconductor Devices and Integrated Circuits—NASECODE V*, (J. J. H. Miller Ed.), pp. 87-92, Trinity College, Dublin, Ireland, Boole Press, 1987.
[23] L. Andór, H. P. Baltes, A. Nathan, and H. G. Schmidt-Weinmar, "Numerical modeling of magnetic-field-sensitive semiconductor devices," *IEEE Trans. Electron Devices*, vol. ED-32, pp. 1224-1230, 1985.
[24] M. S. Mock, *Analysis of Mathematical Models of Semiconductor Devices*. Dublin, Ireland: Boole, 1983.
[25] T. T. H. Pian, "Element stiffness matrices for boundary compatibility for prescribed boundary stresses," in *Proc. Conf. Matrix Methods in Structural Mechanics*, pp. 457-477, Wright-Patterson Air Force Base, OH, 1966.
[26] J. D. Jackson, *Classical Electrodynamics*. New York: Wiley, 1975.
[27] M. R. Pinto, "The influence of spatial discretization of current accuracy," private communication.

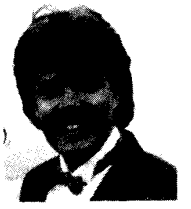

Josef Bürgler received the Dipl. Phys. degree from the Swiss Federal Institute of Technology (ETH), Zurich, Switzerland, in 1982.

Since then he worked as a researcher in the Integrated Systems Lab at the Swiss Federal Institute of Technology where he is currently working towards a Ph.D. degree.

Randolph E. Bank was born in Pittsburgh, PA, on September 13, 1949. He received the B.S. degree in chemistry from the University of Denver, Denver, CO, in 1971 and the M.A. and Ph.D. degrees in applied mathematics from Harvard University, Cambridge, MA, in 1972 and 1975, respectively.

From 1975 to 1981 he held academic positions at the University of Chicago, Chicago, and the University of Texas, Austin, and a visiting position at Yale University, New Haven, CT. In 1981, he became a member of the mathematics faculty at the University of California, San Diego. His main research interest is the study of numerical algorithms for solving partial differential equations.

Dr. Bank is a member of SIAM.

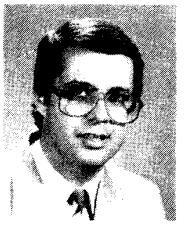

Wolfgang Fichtner (M'79-SM'84) received the Dipl.Ing. degree in physics and the Ph.D. degree in electrical engineering from the Technical University of Vienna, Vienna, Austria, in 1974 and 1978, respectively.

From 1975 to 1978, he was an Assistant Professor in the Department of Electrical Engineering, Technical University of Vienna. From 1979 through 1985, he worked at AT&T Bell Laboratories, Murray Hill, NJ. Since 1985 he is Professor and Head of the Integrated Systems Lab at the Swiss Federal Institute of Technology (ETH).

R. Kent Smith received the B.S. degree in electrical engineering in 1965, the M.S. degree in physics from Bucknell University, Lewisburg, PA, in 1967, and the Ph.D. degree from the University of Maryland, College Park, in 1972.

From 1972 to 1975 he was an Alexander von Humboldt Fellow at the Institüt für Theoritische Physik, Frankfurt, Germany, and from 1975 to 1979 he was Assistant Professor of Physics at Duke University, Durham, NC. Since 1979 he has been with AT&T Bell Laboratories, Murray Hill, NJ, where he is engaged in the numerical simulation of semiconductor devices.